XIII International Conference on Computational Plasticity. Fundamentals and Applications
COMPLAS XIII
E. Oñate, D.R.J. Owen, D. Peric and M. Chiumenti (Eds)

MODELLING THE RESIDUAL STRESS OF AUTOFRETTAGED THICK-WALLED COMMON RAILS USING ISOTROPIC AND KINEMATIC METAL PLASTICITY MODELS COMPARED TO X-RAY DIFFRACTION ANALYSIS

SEBASTIAN ROGOWSKI*

*Volkswagen AG
Component Developement HME
Letter box 7359, P. O. box 31 11 76, 38231 Salzgitter, Germany
E-mail: sebastian.rogowski@volkswagen.de

Key words: X-ray diffraction, FEM, Autofrettage, Common Rail, Computational Plasticity, Validation

Abstract. The pressure in Diesel injection parts is continuously rising up to more than 2500 bar [1]. Especially the Common Rail as the pressure storage of the injection system is in focus of the recent technology development. To help improve the load capability of the component part it is submitted to the process of autofrettage [2]. During the autofrettage process an internal high pressure load causes plastic deformation in some zones of the steel. Relaxing the internal pressure, the resulting elastic hoop induces residual compressive stress in the inner plastically deformed volume [3]. To exactly dimension the depth of this zone it is essential to know the residual stress situation after the autofrettage treatment. Using the integrated plasticity models in ABAQUS® two material models in the FEM were compared at Volkswagen. Results at different autofrettage pressures are computed for a multilinear isotropic material model and a cyclic hardening kinematic-isotropic model (Lemaitre-Chaboche, 1990) [4], both based on experimental results. The validation of these computations is done via X-ray diffraction analysis for a number of positions starting on the interior surface and continuing into the material. The manufacturing and measurement procedures induce path dependent material situations. Because of this it is mandatory to model the dissected component part in the FEM before any valid comparison of residual stresses, X-ray diffraction analysis versus FEM results, can be made. As a result it can be shown that the kinematic-isotropic material model is more appropriate to reproduce the autofrettage process.

1 INTRODUCTION

Modern diesel engines use the common rail injection system. In this system, the operating pressure is separate from the pressure generation. This is an effective way to control diesel injection, thereby reducing exhaust gas emissions [5]. The injection pressure has a substantial impact on fuel consumption. Nowadays the fuel rail, which is a reservoir for injection pressure, has to be capable of withstanding increasing pressures which may exceed 2500 bar [1]. Thanks to the use of materials that are suitable for producing the fuel rail on a large scale, the autofrettage process is applied. One-off plastic deformation through the application of high internal pressure generates residual compressive stresses in the plasticised material zones of the thick-walled component. This increases the tolerable operating pressure and the durability of the fuel rail. Plasticisation can begin in certain areas where notches are found, such as the bore intersections. The area of residual compressive stress stretches to a depth of several millimetres inside the component and depends on the autofrettage pressure, the geometry of the component, the characteristics of the material and the remaining elastic material zones. The material is subject to a direction-dependent load during the autofrettage process. This triggers the Bauschinger effect, which has an impact on rigidity [2, 6, 7]. Additionally, certain types of steel may display anisotropic behaviour as a result of the metal forming processes used on the production line [7]. In order to make an accurate statement from the FE simulation about the residual stress state following the autofrettage process, the material modelling has to be capable of mapping these direction-dependent loads. X-ray diffraction can be used to measure the residual stresses in order to validate the results of the FE simulation.

This investigation compares two material models, one isotropic and one isotropic/kinematic. Each FE simulation is performed using ABAQUS® 6.13-4. The material characteristics for the isotropic model come from tensile tests, while the characteristics for the isotropic/kinematic model come from tensile/compression tests on the component material. The comparison focusses on two component areas that have an impact on rigidity. The first is near a bore intersection, and the second is between two bore intersections. The second area is similar to a thick-walled cylinder. These component areas are important because they are two very different sections of the fuel rail interior. In each case, the FE simulation is validated using two different autofrettage pressures. The fuel rail is mechanically divided in order to measure the residual stresses using X-ray diffraction. This results in a redistribution of the residual stress state, which is modelled in the FE simulation in order to give a useful comparison. This investigation provides validation by comparing the FEA results from the aforementioned combinations of parameters with the results from the X-ray diffraction.

2 METHODS

2.1 AUTOFRETTAGE PROCESS

The autofrettage process is used to create a distinct area of residual compressive stress inside thick-walled components that are subjected to high internal pressure. The component is overloaded using a very high internal pressure, which triggers one-off, targeted plastic deformation. Notch effects cause plasticisation to occur in certain zones of interest such as the

bore intersections. As a result, these areas experience the highest level of plasticisation, and the most distinct area of residual compressive stress can be expected to form here. The result of this process in a thick-walled component is an external, elastically deformed zone which causes pressure in the internal, plastically deformed zone [6, 8]. Figure 1 shows the stress-strain curve during the autofrettage process using a 1D element.

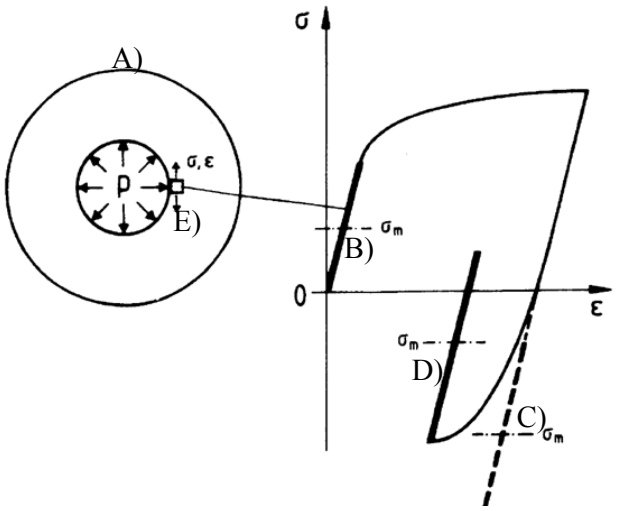

A) Thick-walled pipe under internal pressure
B) Operating load without autofrettage
C) Operating load with autofrettage without kinematic effects
D) Operating load with autofrettage and with kinematic effects

Figure 1: Stress-strain curve for 1D element during autofrettage [8].

This leads to a shift in the average stress σ_m caused by the operating load of the tensile area in the compressive stress area. This has a positive impact on the durability of the component [2, 6, 8].

For this investigation, two different fuel rail samples were manufactured from the same high-strength steel for radiographic analysis of the residual stress state. One was manufactured using an autofrettage pressure of p_{AF} = 11kbar, and the other with p_{AF} > 12kbar. Refer to Table 1 for material characteristics.

Table 1: Material data for the high-strength steel (semi-finished) [9]

Chemical composition in percentage by mass:						
C	Si	Mn	P	S	Cr	Mo
0.28–0.36	<0.50	1.40–1.80	<0.025	<0.040	0.80–1.20	0.25–0.40
Mechanical and technological properties:						
Yield strength $R_{p0.2}$ [N/mm²]			>800			
Tensile strength R_m [N/mm²]			>1150			
Elongation at fracture A [%]			at least 12			
E modulus [MPa]			210000			

2.2 EXPERIMENT – RADIOGRAPHIC DIFFRACTION

Results from the radiographic residual stress measurements were used in order to evaluate the FEM calculations in an independent procedure and to come to a conclusion about the validity of the material model in the FEM calculation. The basic principle of this measuring procedure involves diffracting X-rays through a crystal lattice while changing the elongation of the lattice [10]. The measurements were taken in the plane of the component where the bore intersections are located. This is the most heavily loaded area of the fuel rail [11]. For the purpose of validation, the stresses were therefore calculated tangentially to the main bore. The X-rays penetrate the steel to a depth of approximately 5 µm. The measurements were taken at component depths of up to 1 mm. The focus diameter of 0.8 mm was the size of the measuring spot used for local measurement of the macro residual stresses. Chromium Kα X-rays were used, and the Ψ layout was used for the measuring setup. The $\sin^2\Psi$ technique was used to evaluate the measurements. Electrochemical polishing was used to expose the lattice planes inside the component. The advantage of this etching technique is that it can be used to scrape away material layers without applying any residual stress. Figure 2 shows the measurement position x = 56 mm between two bore intersections and the measurement position x = 2 mm near a bore intersection on the disassembled fuel rail. X is the distance to the central point of the bore intersection near C).

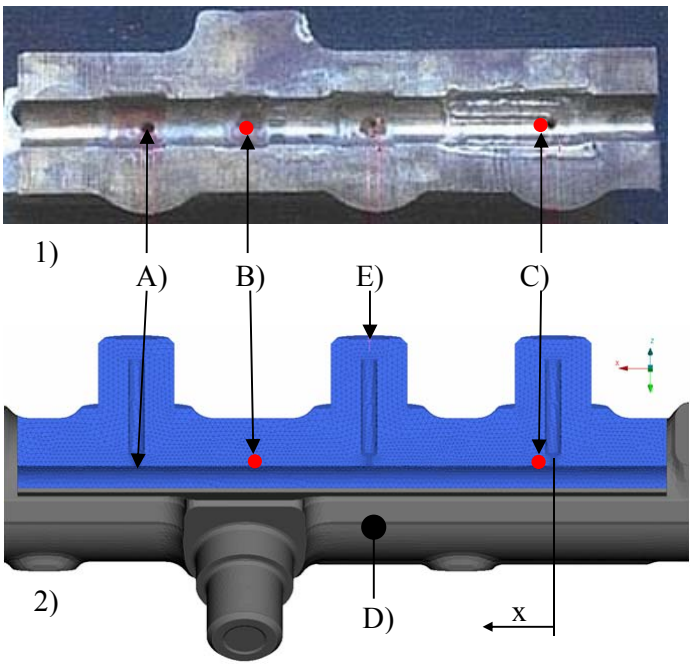

A) Bore intersection
B) Measurement position (red) x = 56 mm
C) Measurement position (red) x = 2 mm
D) Elements removed from FE model (grey)
E) Mount for the part to be measured
1) Part of the fuel rail to be measured
2) Measurement positions shown on the FE model

Figure 2: Measurement positions for the radiographic residual stress analysis on the fuel rail

The measurement method required each autofrettaged fuel rail to be split into two parts by machining. As an example, the resulting part to be measured 1) is shown in Figure 2.

2.3 FINITE ELEMENT ANALYSIS

The static FE model was constructed in such a way that it completes the loading and unloading in the autofrettage process and the separation of the part to be measured in a single calculation. The autofrettage pressure is applied to the element surfaces as a distributed load. The FE model is amended in the next step, when the elements (D) that are not part of the part to be measured in Figure 2) are removed. The forces acting on the contact surfaces of the part to be measured are reduced to zero. During this step in the calculation, the part to be measured is positioned minimally on a single node, which means that the redistribution of the residual stresses remains unaffected. Due to the high level of elongation during the autofrettage process, the calculations are geometrically non-linear. The component does not have a plane of symmetry and was treated as a single piece in order to provide the best possible model of the actual process. The 3D FE model was made from fully integrated continuum elements (tetrahedron, C3D10) and has 1.1 million nodes. Two different material models were used to perform a calculation on the fuel rail that was split to form the part to be measured. The isotropic material model is used in ABAQUS® (hardening=isotropic), in which the prepared test data for tension and elongation from the tensile test are entered in table format. These are tabulated up to a tensile strength of approximately 1290 N/mm² at 5 % elongation. For the isotropic/kinematic material model (hardening=combined), tensile/compression tests are carried out up to a maximum elongation/compression of approximately 5% and the results are used to calculate the material parameters. These parameters are entered into ABAQUS® using a model developed by Lemaitre and Chaboche in 1990 [12].

Isotropic model

The isotropic material model describes the plasticity of the material when the yield surface, i.e. the yield strength, increases uniformly in all directions. If, on the basis of this model, a single-axis tensile/compression test initially achieves the maximum plastic tensile stress, the yield strength for the subsequent compression load corresponds to the maximum tensile stress achieved [13, 14]. This means that, following the application of an initial, quick plasticising load, the yield point is greater in value than the yield strength of the material in its original state.

Isotropic/kinematic model

Kinematic hardening alters the yield surface solely in terms of its position in the stress space. As a result, the material becomes anisotropic [14]. The model used in this investigation combines isotropic and kinematic hardening. The required material parameters were taken from tensile/compression tests. The parameters generated using a backstress term ($\bar{\sigma}_0, Q_\infty, b, C, \gamma$) were calculated using curve fitting. A detailed mathematical description of this model can be found in [4] and [12]. By using this material model in the FE calculation, it is possible to account for the direction-dependent behaviour of the component material (Bauschinger effect, anisotropy) during the autofrettage calculation.

Validation of the residual stress values from the results of the FE calculations uses conditions equivalent to those used for the radiographic residual stress measurements. In this process, the stress values are determined as an integral mean value over the focus diameter of 0.8 mm.

3 RESULTS

Figure 3 shows the results of the FE calculations for the autofrettage process (p_{AF} > 12000 bar) and the subsequent redistribution of the residual stresses caused by dismantling the part to be measured. The residual stresses tangential to the main bore are displayed in colour (area: 1300 MPa to -1300 MPa). These are stresses in the φ-direction (using the local, cylindrical coordinate system).

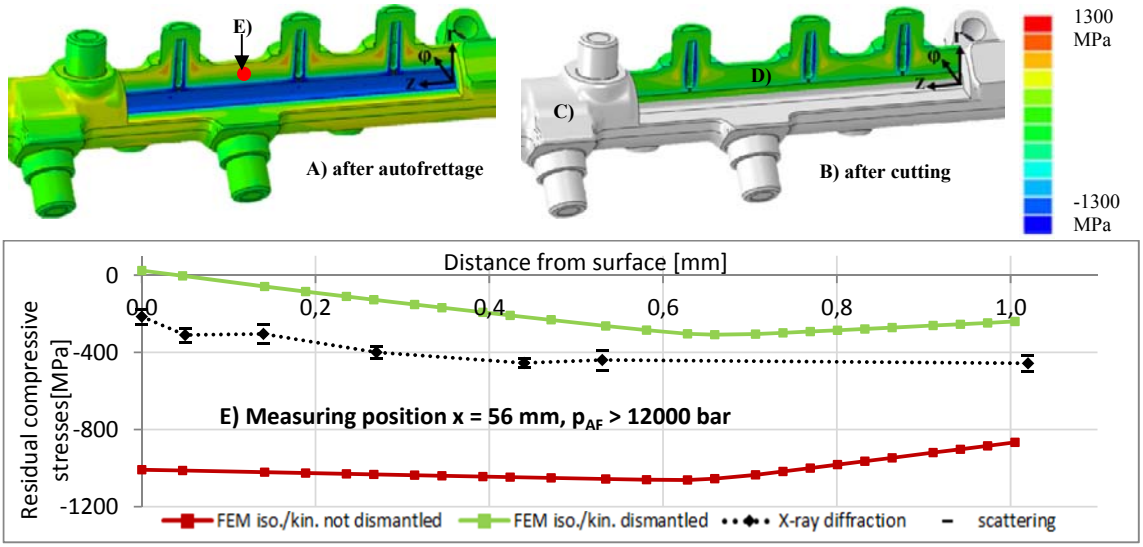

Figure 3: Results of the FE calculation (p_{AF} > 12000 bar)

The distinct area of residual compressive stress in the inner zones and at the bore intersections after autofrettage is clearly visible (cf. Figure 3 A), blue areas). The redistributed residual stress state can be seen clearly in Figure 3 B), as compared to A). On average, the area of residual compressive stress is reduced by more than 600 MPa up to a distance from the surface of 1 mm. The areas removed during the separation phase can be seen in Figure 3C). Figures 4, 5, 6 and 7 below show the residual tangential stresses across the depth of the electrolytic removal, and the distance from the surface, using the cylindrical coordinate system introduced in Figure 3. The FEM results have been extracted from Section D) of Figure 3.

Figure 4 clearly shows that the results of the isotropic/kinematic FE calculation over the various distances from the surface run parallel to the stress values from the radiographic residual stress measurement. The comparatively low level of residual compressive stress in the isotropic/kinematic FE calculation can be seen clearly. The difference between the radiographic measurement and calculation (iso/kin) is approximately 200 MPa. The results

from the FEM material models (Figure 4, green and blue) run in opposite directions up to a distance from the surface of 0.5 mm. Up to this distance, the residual compressive stresses are much greater in value in the isotropic model. The results for both material models are closer when the distance from the surface is 1 mm.

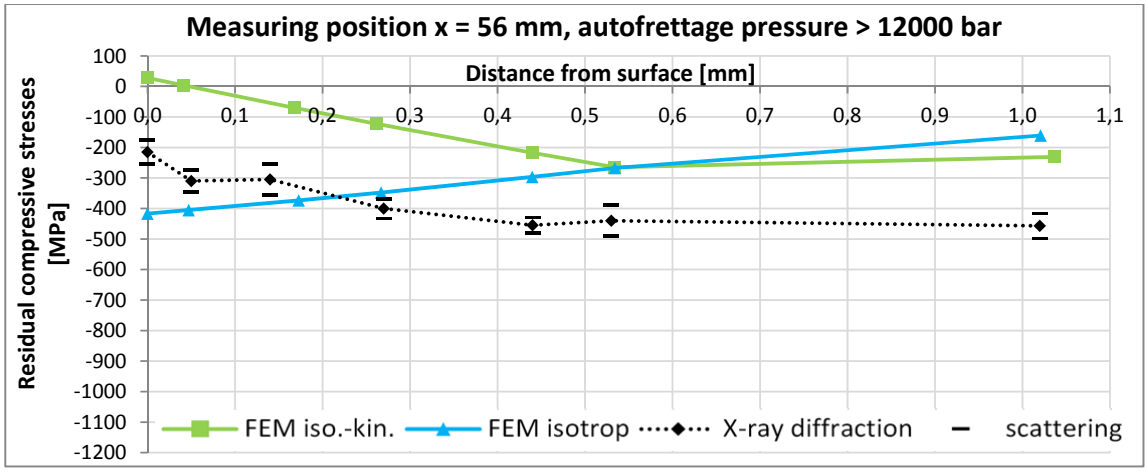

Figure 4: Residual compressive stresses; two FEM material models versus X-ray diffraction; p_{AF} > 12000 bar; x = 56 mm

Figure 5 shows a discrepancy between the qualitative progression of both FE calculations and the radiographic residual stress measurements. The results from the isotropic/kinematic model are clearly more closely aligned with the radiographic measurements.

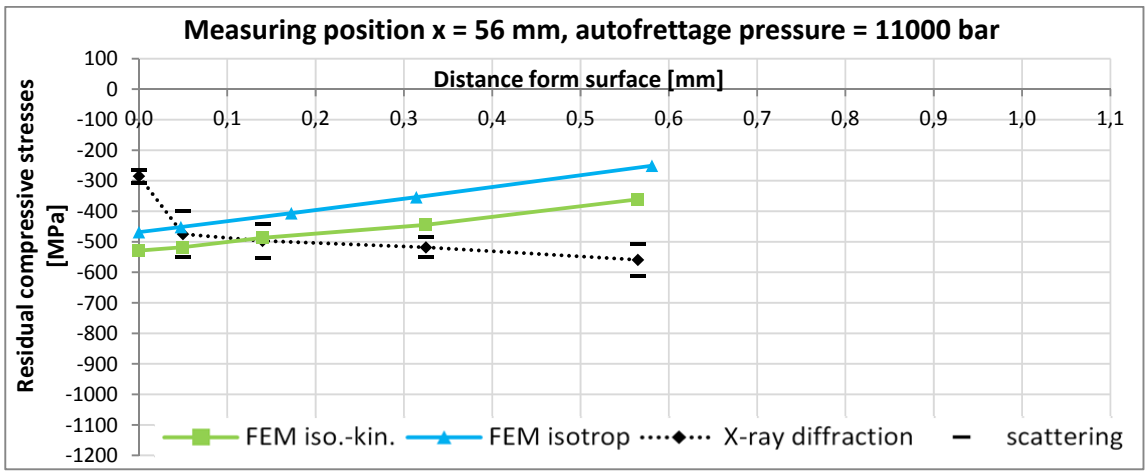

Figure 5: Residual compressive stresses; two FEM material models versus X-ray diffraction; p_{AF} = 11000 bar; x = 56 mm

As in Figure 4, Figure 6 shows values for $p_{AF} > 12$ kbar, but with a different measurement position. The continuing discrepancy compared to the radiographic measurements is clear, as is the tendency towards a progression similar to the radiographic measurements in the isotropic/kinematic FEM as the distance from the surface changes.

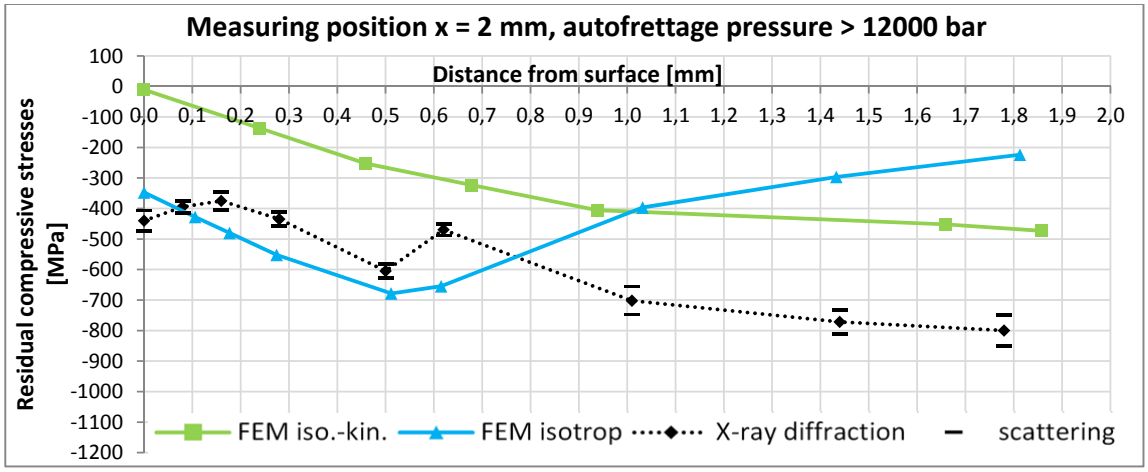

Figure 6: Residual compressive stresses; two FEM material models versus X-ray diffraction; $p_{AF} > 12000$ bar; x = 2 mm

Figure 7 confirms the trend for changing distance from the surface for $p_{AF} = 11$ kbar shown in Figures 4 and 6. The isotropic/kinematic FEM results for the three measurements closest to the surface are within the scatter range of the radiographic residual stress measurements.

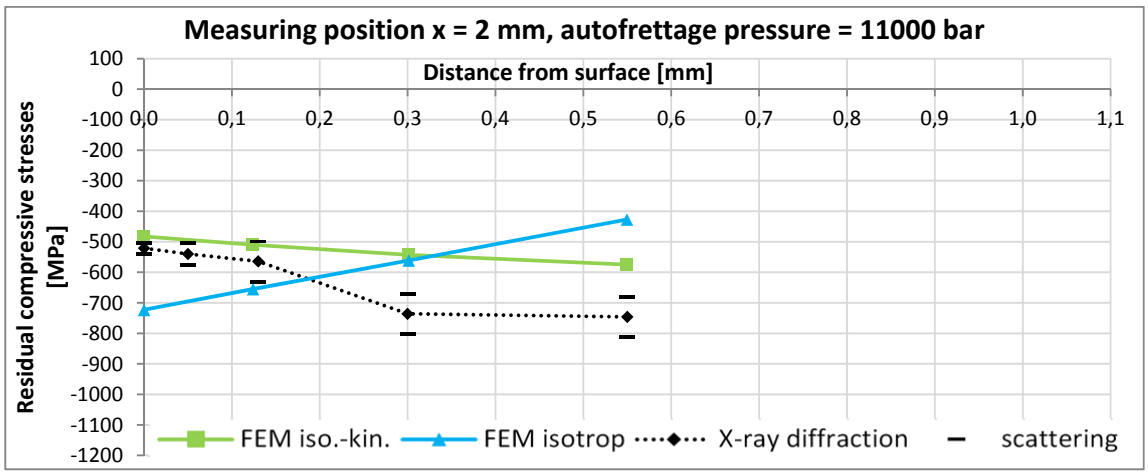

Figure 7: Residual tangential stresses; two FEM material models versus X-ray diffraction; $p_{AF} = 11000$bar; x = 2 mm

The scatter of the individual radiographic measurements is a minimum of 18 MPa and a maximum of 75 MPa, where the arithmetic mean of the scatter is 35 MPa for $p_{AF} > 12$ kbar and 49 MPa for $p_{AF} = 11$ kbar.

4 DISCUSSION

The results from the radiographic diffraction have been used to validate the residual stresses calculated, in each case in the φ-direction of the coordinate system in Figure 3. To achieve a meaningful comparison, the sample preparation step which affects the redistribution of the residual stresses was modelled in the FEA. By way of comparison, refer to Figure 3 B) and [6] page 933 ff. These clearly indicate that splitting components that are under global residual compressive stress leads to a considerable reduction of these stresses at a local level. A statement about the validity of the models is therefore only possible if this preparation step is taken into account. The FEA results from the isotropic/kinematic material model display a stress curve that is equivalent to the results of the radiographic measurements across all measurement areas and configurations. See Figures 4, 6 and 7. Furthermore, the results calculated on the basis of the purely isotropic material model demonstrate that the residual compressive stresses near the surface have potentially been overestimated. By way of comparison, refer to the values up to a distance of approximately 0.3 mm from the surface in Figures 4 and 7 and [6], page 926 ff. For this reason, the isotropic/kinematic material model developed by Lemaitre and Chaboche in 1990 [4, 12, 13] can be considered valid for the static FEM calculation of the autofrettage process in thick-walled tubular components.

5 CONCLUSION

This investigation demonstrates a methodology for evaluating two different material models for the FEM calculation of the autofrettage process on a fuel rail using radiographic residual stress analysis. The investigation also clarifies the impact of direction-dependent material effects on the material models used. In conclusion, it is shown that an isotropic/kinematic material model developed by Lemaitre and Chaboche is valid for reproducing the residual stress state in certain, potentially important component areas. However, the model parameters have to be extended in order to achieve a more accurate reproduction of the residual stresses using FEM. In his paper on the *Deformation and Damage Behaviour of Metallic Materials*[...], *Döring* [4] recommends using multiple backstress terms to provide more grid points for the material model while determining the parameters from the test dataset.

6 ACKNOWLEDGEMENT

The author would like to thank Dr. A. Gitt-Gehrke and Mr. H. Hartung at Volkswagen AG and Dr. M. Bäker at Technical University Braunschweig for the inspiring discussions. The author also gratefully acknowledges the technical support of Mr. A. Janke and Mrs. N. Zigic from the Component Development at Volkswagen AG.

REFERENCES

[1] Robert Bosch GmbH, Diesel Systems – Common Rail Systems CRSN3 with 2,000 to 2,500 bar, www.future-with-diesel.com, 292000P0WJ-C/CCA-201302-En, Stuttgart, 2013.

[2] R. Thumser, Simulation des Rissfortschritts in autofrettierten und nicht autofrettierten Bohrungsverschneidungen auf der Grundlage der linear-elastischen Bruchmechanik. Dissertation, Bauhaus-Universität Weimar, 2009.

[3] M. Maleki, G.H. Farrahi, B. Haghpanah Jahromi, E. Hosseinian, Residual stress analysis of autofrettaged thick-walled spherical pressure vessel. International Journal of Pressure Vessels and Piping, 87:396-401, 2010.

[4] R. Döring, Zum Deformations- und Schädigungsverhalten metallischer Werkstoffe unter mehrachsig nichtproportionalen zyklischen Beanspruchungen. Veröffentlichung des Instituts für Stahlbau und Werkstoffmechanik der Technischen Universität Darmstadt, Heft 78, 2006.

[5] K. Reif, Dieselmotor-Management, Systeme, Komponenten, Steuerung und Regelung. Heidelberg, Springer-Verlag, 2012.

[6] H. Brünnet, I. Yi, D. Bähre, Modeling of Residual Stresses and Shape Deviations along the Process Chain of Autofrettaged Components. Journal of Materials Science and Engineering, A 1:915-936, 2011.

[7] H.-J. Bargel, G. Schulze, Werkstoffkunde. Berlin, Heidelberg, New York, Springer-Verlag, 2012.

[8] T. Seeger, Autofrettage 1, Vorhaben Nr. 478, Dauerfestigkeitssteigerung durch Autofrettage, Abschlussbericht. FVV Forschungsheft, 1993.

[9] Saarstahl AG, Produktinformation, Werkstoff-Datenblatt, 2014

[10] P. Spieß, G. Teichert, R. Schwarzer, H. Behnken, C. Genzel, Moderne Röntgenbeugung, Röntgendiffraktometrie für Materialwissenschaftler, Physiker und Chemiker. Wiesbaden, GWV Verlag GmbH, 2009.

[11] M. Lechmann, Entwicklung eines schwingbruchmechanischen Auslegungskonzeptes für innendruckbeanspruchte Bauteile mit ausgeprägten Druckeigenspannungsfeldern, Dissertation. Universität Stuttgart, 2007.

[12] Dassault Systemes, Abaqus 6.13 – Theory Guide, 2013

[13] Dassault Systemes, Abaqus 6.13 – Analysis User's Guide, 2013

[14] J. Rösler, H. Harders, M. Bäker, Mechanisches Verhalten der Werkstoffe. Wiesbaden, Springer Vieweg, 2012.